

Impact of Internal Waves on the acoustic field at a Coastal Station off Paradeep, East Coast of India

B.Sridevi, T.V.Ramana Murty*, Y.Sadhuram and V.S.N.Murty

National Institute of Oceanography (CSIR), Regional center, 176, Lawsons Bay colony

Visakhapatnam-530 017, India.

E-mail: *tvrmurty@nio.org

Abstract

Internal Wave (IW) characteristics and the impact of IW on acoustic field have been studied utilizing the hourly time series of temperature and salinity data collected at a coastal site off Paradeep (North Bay of Bengal) during 24 - 25 October 2008. The IW characteristics, viz; period (t_{per}), velocity (C_{vel}), wavelength (L) and wave numbers (k) are found to be 2.133 hrs – 34.72 hrs, 0.135 km hr⁻¹, 0.37 km - 6.2 km and 2.70 - 0.16 cycles km⁻¹ respectively. The semi-diurnal tidal forces are predominant than diurnal as well as at other frequencies and its contribution is about 64% towards the total potential energy ($E_0 = 3.34 \text{ J m}^{-2}$). Sound velocity perturbations with space and time in the presence of IW field are examined from Garrett-Munk (GM) model. Transmission loss anomaly for optimized source-receiver configuration at the depth of 53 m and range of 9 km has been computed from acoustic modeling. The loss in the acoustic transmission is found to be 38.4 dB in the presence of Low frequency IW field.

Key words: Internal waves, Garrett-Munk model, acoustic modeling, ray paths,
Bay of Bengal

1. Introduction

Physical variability occurs in the ocean with space (scales of millimeters to planetary) and time (from seconds to geological times) due to external and internal forcing (Robinson and Ding Lee, 1994). Physical oceanographers are interested to study the variability of ocean environment (of different spatial scales: global – basin – subbasin – mesoscale – submesoscale – fine and microstructure) rather than it's mean. To monitor ocean variability, acoustic principle is adopted. In ocean-acoustic modeling almost all the effects of oceanic volume changes are accounted for by the changes in the ocean sound velocity, or equivalently, by changes in the index of refraction. It is well known that in the ocean, sound (in contrast to light) is the only viable means for communication and range finding and also synoptically probing of above oceanic features. Sound can fulfill all the three requirements: (1) penetrative range is more, (2) high resolving power, and (3) high velocity of transmission. For monitoring the above features and their impact on sound propagation, acousticians usually conduct the experiments to measure the travel time and amplitudes of sound pulses between sound sources and receivers distributed at suitable locations in the ocean (Ramana murty and Mahadevan, 1994). In this technique we assume a reference ocean stratified in the vertical direction, and trace the sound ray paths from a source to a receiver. For this simulation, the local climatological (or insitu) mean state of the ocean could be used as the reference state. Indeed it can be justifiably stated that in the large majority of ocean-acoustic models, the only link between the acoustics and the oceanography is via the sound velocity. Oceanic changes relevant to underwater acoustics are classified into mean and fluctuating components (De Santo, 1979) with the following general model of the sound velocity equation

$$C(r, t) = C_o(z) + \delta C_1(r) + \delta C_2(r, t) \quad \dots\dots\dots (1)$$

z – depth, t – time, r – three dimensional position

having characteristics: 1) a mean vertical profile $C_o(z)$ that represents local climatology ($C_o \sim 1500 \text{ ms}^{-1}$), 2) a meso scale component ($\delta C_1(r)$) (fronts, eddies) -- deterministic with respect to the acoustic time scale ($\delta C_1 / C_o \sim 10^{-2}$), and 3) a time-varying component ($\delta C_2(r, t)$) (i.e small scale time varying component with respect to the acoustic time scale, $\delta C_1 / C_o \sim 10^{-4}$) that represents small scale fluctuations caused by Internal Waves (IW) of fine and microstructure. At typical sonar operating frequencies, the

main cause of these fluctuations ($\delta C_2(r,t)$) are IWs. These can be strong enough to completely prevent a signal from being detected. Of the oceanic fluctuations categorized in the above, the smaller scale statistical component fluctuations ($\delta C_2(r,t)$) occur on temporal and spatial scales more comparable to the acoustic scale. These fluctuations would affect the coherence with space and time of repeated acoustic measurements done by acousticians. These fluctuations ($\delta C_2(r,t)$) and their effect on ocean acoustics that we will examine with insitu time series observations off Paradeep to have pre-requisite information before conducting the actual experiment. Signatures of IW characteristics of ($\delta C_2(r,t)$) can be deduced by collection of continuous records of environmental time series data from current meters having proper choice of sampling interval (viz., sample interval is 1-5 minutes) and CTD data to derive stratification of the water column.

In a stratified medium, a fluid displaced from its equilibrium level experiences a restoring force proportional to reduced gravity and the disturbance propagates in the form of an internal wave (IW). This oscillating motion in the interface layer is described as an IW and does not affect the surface. Study on IW has many applications which include: Military (submarine navigation) and Civilian (pollution monitoring, power generation, offshore oil drilling operations) and also play a major role in ocean thermodynamics. In view of these aspects, many researchers identified the IWs from SAR images (Xiaofeng Li, *et al*, 1999), shipboard Radar (Dong-Jiing Doong *et.al*, 2007), special instrumentation like Isothermal follower and thermistor chain (Garrett and Munk, 1979). An insight into IWs in the seas around India has been broadly described by Murthy (2002). In the recent past some studies were done on IWs in the seas around India utilizing the time series measurements from stationary ships and from the oceanographic buoys in the Arabian Sea (Murthy and James, 1996; Murthy and Mohan Kumar, 1996; Krishna Kumar and Murthy, 1998). Most of these studies revealed the IW parameters like amplitudes, frequencies, speeds and directions, wavelengths, etc., and their variability with space and time. Such studies have not been done in the Bay of Bengal which may be due to lack of data. It is too expensive and tedious job to get the IW field with space and time. Simulation technique provides alternative to direct observations for generating large amounts of synoptic data over specified ranges and resolutions. However the simulations can never replace the direct measurements, rather supplement them. In the present study, we have attempted to simulate random linear IW field δC_2 from source using modified GM model (Dirk

et.al, 1997) from the time series CTD data was collected by SBE 19 plus seacat profiler (Make Seabird electronics, USA) at a depth of 130 m off Paradeep in the north Bay of Bengal (Fig.1). The GM model incorporates more observational data than any other model and has been widely accepted by the scientific community worldwide. GM model can generate IW field with space and time from the time series data at a fixed location, which will be useful to run acoustic model and these results are useful to naval operations. The sound velocity perturbations at different depths (computed from CTD time series data off Paradeep) as reproduced from the GM model at specified ranges due to these IW are utilized to estimate the changes in the acoustic transmission loss with the ray model which is useful for navy for under water communication.

2. Data and Methodology

Time series CTD data at hourly interval at a depth of 130 m (shown as diamond in Fig.1) collected off Paradeep, East Coast of India during 24 – 25 October 2008 have been used to study the IW characteristics.

2.1 IW Characteristics

Typical vertical scales of IW are around 10 m and the horizontal scales vary from few hundreds meters to kilometers. Temporal scales are of the order of hours, bounded by a minimum frequency at the inertial frequency (ω_i) (a function of latitude) and a maximum frequency at the Brunt-Vaisala frequency ($N = \sqrt{\frac{-g\partial\rho}{\rho\partial z}}$). With in the above frequencies, IW characteristics like amplitudes, velocities, wave length, wave number, energies were computed following the earlier studies (Defant, 1961; Murthy and Murthy, 1986; Stephen, 2000). The waters in the pycnocline are stratified i.e., least turbulent. When these waters are disturbed by an external force (winds, surface waves, tides, etc) and internal force (shear associated with currents, bottom force etc) they respond through manifestation of IW.

One of the required parameters for the simulation of IW by GM model is wave number ($k = 2\pi / L$, $L = C_{vel} t_{per}$, where L, C_{vel}, t_{per} are wave length, velocity and period respectively. To compute L, C_{vel} and t_{per} are needed. C_{vel} is computed using two layer density model (Defant , 1961) as $C_{vel}^2 = gh(\rho - \rho') / \rho$ where h is the thickness of the top layer of weak density

gradient, ρ is density of bottom layer of strong density gradient ρ' is the mean density of top layer of weak density gradient and g is the acceleration due to gravity. Here we have considered wave number domain (k) (Sridevi *et al.*, 2010) instead of frequency domain (ω_i) (Krishna Kumar and Balasubramanian, 2005). An insight into IWs in the seas around India was reviewed by Murthy (2002) and found that the IW frequencies extending from inertial frequency to semidiurnal frequency – internal tides - dominate the low frequency (LF) band of IW, while IW of > 0.5 cph (0.005 hrs) dominate the high frequency (HF) band of IW i.e., in terms of wave number (k) range LF IW field is found to be 0.02 cycles km^{-1} to 0.91 cycles km^{-1} . In the present study, the simulation is confined to study the impact of LF IW field on sound propagation. Another parameter required for GM model is energy factor (E_o) which can be estimated from the in-situ time series data. In order to compute E_o , amplitudes and phases of IWs are needed. For this purpose, the temperature ($T(z,t)$) and vertical displacement ($\eta(z,t)$) of pycnocline due to IW expressed in terms of ensemble mean $\bar{T}(z)$, tidal constituents (ω_i) are estimated following Stephen (2000):

$$T(z,t) = \bar{T}(z) + \sum_{i=1}^n T_i(z) \cos(\omega_i t - \phi_i^T(z)) \quad \dots\dots\dots(2)$$

$$\eta(z,t) = \sum_{i=1}^n \eta_i(z) \cos(\omega_i t - \phi_i^\eta(z)) \quad \dots\dots\dots(3)$$

where z is the depth array, t is the time array, n is the number of tidal frequency. The vertical displacements for each tidal constituent can be estimated by dividing the amplitude functions by the vertical gradient i.e., $\eta_i(z) = T_i / (\frac{\partial \bar{T}}{\partial z})$. The functions of $\phi_i^T(z)$ and $\phi_i^\eta(z)$ represent phases corresponding to temperature and displacement. Once amplitudes and phases of displacement function ($\eta(z,t)$) of IWs are computed, E_o [= Potential Energy (PE) + Kinetic Energy (KE) + Baroclinic potential energy (BPE)] can be estimated (Stephen, 2000).

$$\langle PE \rangle = \frac{1}{2T} \int_0^T \rho g \eta^2(t) dt \text{ and} \quad \dots\dots\dots (4)$$

$$\langle KE \rangle = \frac{1}{2T} \int_0^T \rho H (u^2(t) + v^2(t)) dt \quad \dots\dots\dots (5)$$

$$\langle BPE \rangle = \frac{1}{T} \int_0^T \frac{1}{2} \int_{-H}^0 \rho(z) N^2(z) \eta^2(z,t) dz dt \quad \dots\dots\dots (6)$$

where $\eta, u, v, T, \rho, H, N$ are the displacement profile, zonal and meridional currents, observational period, density, water depth and Brunt-Vaisala frequency respectively. Here $\langle \rangle$ indicates ensemble average. Equations (4-6) have been performed by cubic spline method (Ralston and Wilff, 1967). Apart from above parameters, stratification scale (B) and extrapolated parameter (N_o) are also needed for GM model and can be computed from formulae $N(z) = N_o e^{-z/B}$. The least square method adopted for the data $N(z)$ to obtain parameters (B) and (N_o). The value of B is 0.129 km. The value of $N_o = 0.029 \text{ cph}$ has been taken as inertial frequency (Krishna Kumar and Murty, 2002).

2.2 Modeling of Internal Waves

Simulation may be defined as the process by which a realistic field of oceanographic variables is generated. Such oceanic environment simulations are required to be used in systems design, system performance evaluation and basic research.

The IW parameters vary with space and time. Their measurements at sea are too expensive. Therefore successful modeling of IW provides the IW parameters at any interested site in the sea. Garrett and Munk (1975) succeeded in modeling deep water IW-GM model – and later improved it for the shallow water IW, (Munk, 1981). This GM model takes the input of mean sound velocity ($C_o(z)$) (back ground) profile of time-series data at a fixed position as

initial condition and generates the fluctuations of sound velocity due to IW with space and time ($\delta C_2(r, t)$) neglecting other fluctuations ($\delta C_1(r)$). More details can be found in Krishna Kumar and Balasubramanian (2005) and Flatte. *et. al*, (1979). IW eigen-frequencies (ω_j^2) and modes ($W_j(z)$) at a specified sequence of horizontal wave numbers (Table1) are computed using “finite difference – Sturm sequence – bisection – inverse iteration method” (Carnahan *et.al.*, 1969), with mean profiles ($N(z)$) deduced from CTD data following the equation,

$$\frac{d^2 W_j(z)}{dz^2} + \left\{ \gamma_j^2 [N^2(z) - \omega_l^2] - k^2 \right\} W_j(z) = 0 \quad 0 \leq z \leq H \quad (7)$$

where $W_j(0) = W_j(H) = 0$ and k is a known spatial wave number in rad m^{-1} . The quantities $\gamma_j^2, j=1, J$ are the eigen values that are related to the eigen-frequencies by the equation $\omega_j^2 = \omega_l^2 + k^2 / \gamma_j^2$ (Dozier and Tappert, 1978).

From these model calculations, sequences of sound speed realizations ($\delta c_2(r, z, t)$) based on the input temperature and salinity (Munk and Zachariasen 1976) are obtained using the GM IW spectrum model (Flatte *et.al* 1979) defined by,

$$\delta c_2(r, z, t) \cong (dc_p / dz) \text{Re} [\zeta(r, z, t)] \quad (8)$$

where, dc_p / dz is the potential sound speed gradient in (s^{-1}) and $[\zeta(r, z, t)]$ is the IW displacement function is given by,

$$\zeta(r, z, t) = \sum_{j=1}^J \int_{-\infty}^{\infty} A_j(k) W_j(k^2, z) \exp[ikr + i\omega_j(k^2)t] dk \quad (9)$$

where the k^2 dependence of the internal wave modes and eigen-frequencies are indicated explicitly. The expansion coefficients $A_j(k)$ are identically distributed complex Gaussian random variables with zero mean. Their variance is given by the Garrett-Munk power spectrum defined by Flatte', *et. al.* (1979) as

$$P_j(k^2) = E_0 \frac{4}{\pi^2} \frac{3}{j^2 + j_*^2} \frac{k_j k^2}{(k^2 + k_j^2)^2} \quad (10)$$

where $k_j = (\pi F_I / BN_0)j$, B the stratification scale, (Ramana Murty *et.al.*, 1989), N_0 extroploated Brunt-vaisala frequency and E_0 the energy density factor. The quantity F_I is the inertial frequency computed using $F_I = (1/12) \sin(\text{latitude})$ with units in cph. Using temporal and spatial distribution of sound speed realizations, the range-independent and range-dependent numerical ray tracing experiment is conducted to obtain eigen rays and transmission losses etc., to study the impact of IWs on sound propagation.

3. Results and Discussions

The depth-time section of temperature ($^{\circ}\text{C}$) at the fixed location (Fig.1) is presented in Fig.2. The temperature of the top layer is quite warm ($> 29^{\circ}\text{C}$) during the observational period. The mixed layer is shallow (about 17 m). Strong oscillations in the thermocline indicate the presence of internal waves. The near-diurnal cycle of 10 hr period is evident with the shoaling of isotherms at 0900 hrs and 1900 hrs on 24th October and again at 0700 hrs on 25th October. With depth, the occurrence of diurnal peaks lagged by a few hours from that at 40 m depth. The depth-time section of salinity in the upper 100 m water column at the time series location shows the occurrence of fresh water plume, characterized by low saline (< 30 psu) waters (Fig. 3). The isohalines in the halocline layer, in the depth range of 10 m – 35 m, show the dominant semi-diurnal oscillation of 12 hours period. This semi-diurnal wave period is slightly longer than that of semi-diurnal cycle of temperature (Fig. 2). Below the halocline, the semi-diurnal peaks occurred after 3 hours. The IWs are not discernible in the mixed layer. The presence of warm and fresh waters in the mixed layer and the cold, saline waters contributed to the intense stratification and hence density gradients in the upper ocean. The prevailing northeasterlies (winds blowing from northeast) might contribute to the generation of IWs in the thermocline.

The sound velocity structure shows a subsurface maximum below the mixed layer and within the halocline and the isolines of sound velocity also suggest the presence of IWs (Fig.4). The ensemble mean profiles of temperature, salinity, sound velocity, Brunt-Vaisalla frequency (N^2) are presented in Figure 5. The MLD is found to be 40 m. From the temperature profile, it is seen that it is varied between 28°C to 22°C . A strong gradient in the top layer is seen in the salinity profile which was varying from 29.5 psu at surface to 33.5 psu at the depth of 40 m and then it is linearly increasing up to the bottom. The sound velocity profile has subsurface duct

up to 40 m and below that it is decreasing and following the temperature profile. The Brunt-Vaisalla frequency profile has a peak value of 29.5 cph at depth of 25 m. The above parameters derived from the CTD data are used to examine the tidal forcing on displacement function $\eta(z,t)$ (Fig. 6) which indicates the signatures of diurnal and semi-diurnal cycles. By computing the terms at each frequency, the vertical displacements for each tidal constituent can be estimated by dividing the amplitude functions by the vertical gradient i.e. $\eta_i(z) = T_i / (\frac{\partial \bar{T}}{\partial z})$.

The computed amplitudes and phases are shown in Figure 7. From this figure, one can infer that the semi-diurnal tidal forces are predominant than diurnal as well as at other frequencies. The high peaks of amplitudes (3.5 – 12 m) at (frequencies: 0.081, 0.069, 0.109 and 0.029 cph) are observed at depths of 86 and 26 m. Most of the time, phases of diurnal and semi-diurnal are in coherent from surface to 40 m depth and incoherent below that depth (Fig. 7).

It is well known that the IWs within a wide range of frequencies – from short period waves to seconds to IWs with periods of days. Those waves with astronomical tidal periods – the so called baroclinic tides – occupy a central place because they are more intensive and more pronounced in the ocean than most of the others. Calculations of power spectra for various sites of the world ocean have shown that at all locations a peak can be found in the spectral density which is in the vicinity of the tidal frequency. Gregg and Briscoe (1979) estimated that one-third of all vertical displacements can be attributed to baroclinic tides. An analysis by Muller and Briscoe (2000) has confirmed the observation of spectral peaks at the inertial and semidiurnal tidal frequencies. In view of these aspects and to supplement input to GM modal, energies have been computed and presented in Table-1. It has been observed that the estimated total energy (E_o) is 3.34 J m^{-2} . This is almost higher than that observed (1.0226 J m^{-2}) off Bhimilli, of east coast of India (Sridevi *et.al*, 2010). The semi-diurnal (0.08 cph), inertial (0.029 cph) and diurnal (0.042 cph) are predominant energy of all other IW frequencies. It is interesting to note that the contribution of semi-diurnal tide is about 64 %. The BPE is 0.14 J m^{-2} . KE has not been calculated due to lack of insitu current measurements. Using POM model, (Rao *et.al*. 2010) also showed predominate active IW field in the north compare south. This is mainly attributed to the stratification due to fresh water discharge, tidal force and bathymetry (coastal waters off Paradeep is about 12 % shallower compared to that of Bhimilli). Since the diurnal and semidiurnal energies are dominant, the baroclinic tides spread out their

energy to develop spectral distribution, as was first recognized by Garrett and Munk (1972). It is interesting to note that BPE is 0.06 J m^{-2} which is comparable and double to inertial frequency (0.03 J m^{-2}) (Table-1). These energies play an important role in the thermodynamics of ocean and regarded as a source of global ocean energy dissipation due to advection of deep water to be balanced by downward diffusion of heat (Munk and Wunsch, 1998).

3.1 IW simulation

The Buoyancy profile has been generated (Fig. 5) using the observed temperature and salinity profiles on uniform mesh, with a depth increment of $\Delta Z = 2 \text{ m}$ for the purpose of computing the IW modes and eigen-frequencies. In the present model, care is taken to see that the local Brunt-Vaisala Frequency is between 0.029 cph (inertial frequency) to 29.5 cph (maximum frequency) and stratification scale ($B = 0.129 \text{ km}$) (Ramana Murty *et.al*, 1989).

Usually the value of B is 1 km observed for deep tropical waters (Munk and Wunsch, 1979). From our in-situ observations, it is evident that the modes should oscillate between frequencies $\omega_i = 0.029 \text{ cph}$ to $N(z) = 29.5 \text{ cph}$ (at depth 25.5 m) i.e., in terms of wave number (k) given by $0.16 \text{ cycles km}^{-1}$, GM model has its own limitation i.e., the choice of maximum wave number interval ($k_{min} = 0.01$ to $k_{max} = 0.5 \text{ cycles km}^{-1}$) containing the majority of energy in the IW spectrum (Evans, 1992). In the present simulation of IW field, we have taken $k_{min} = 0.029$ and $k_{max} = 0.16 \text{ cycles km}^{-1}$. A wave number sampling increment of $\Delta k = 0.01 \text{ cycles km}^{-1}$ with samples between $0.029 \text{ cycles km}^{-1}$ (lower bound of LF) and to $0.16 \text{ cycles km}^{-1}$ (upper bound of LF) and the same samples at negative wave numbers are consider to compute normal modes. A total of 20 IW modes and eigen-frequencies were computed at each of the above said positive wave numbers. The value of $E_0(3.34)$ computed from the present data was used to generate realizations of displacements in terms of sound velocity fluctuations. Usually $E_0 = 4.0$ is taken for deep water (Flatte', *et.al*, 1979). Here, we have choosen sound velocity profiles rather than temperature and salinity profiles because of their direct utility in sonar range prediction models. Sound velocity profiles (C) were obtained by adding the fluctuations (δC_2) in the following equation (Munk and Zachariasen, 1976) to the background profile (C_0)

$$\delta C_2(r, z, t) \cong (dc_p / dz) \text{Re}[\zeta(r, z, t)] \dots\dots\dots (11)$$

where dc_p/dz is the potential sound velocity gradient, r is the range, z is the depth, t is the time and $\zeta(r, z, t)$ is the IW displacement function. Sound velocity profiles were generated for every 600 sec (10 minutes) between 0 and 3000 Sec (50 minutes) and every 0.1 km between 0 and 9 km. At this range, all the IW frequencies (Table -1) propagate in the media and affect sound propagation. The temporal and spatial dependence of the sound velocity in the LF IW field in the contour form is shown in Figure 8. The range dependence of the sound velocity profile is the most important consequence of the IWs, on the temporal and spatial scales selected. The spatial - independence (Without IWs - WIW) and spatial – dependence (IW) of sound velocity profiles have been used as input (left panel of Fig. 9) to trace the rays between source-receiver configuration at 53 m depth, to compute eigen rays (middle panel of Fig. 9) and their corresponding intensity losses (right panel of Fig. 9) (Ramana Murty *et. al.*, 2005). Generally, there are four classes of rays 1) R/R (purely refracted both above and beneath the axis) 2) SR/R (surface reflected and refracted), 3) R/BR (refracted and bottom reflected) and 4) SR/BR (surface and bottom reflected). From Figure 9, one can conclude that 48 R/R category eigen rays for range-independent and 5 R/R rays for range-dependent are seen among all possible 4 classes. It is interesting to note that the surface and bottom influence are not seen, since sound energy cannot penetrate towards higher refractive media and confined within IW field. While calculating intensity, surface and bottom inputs are not incorporated in the ray model. The travel times are clustered which may be due to the anticipated ray path degeneracy (Munk and Wunsch, 1979). To avoid ray path degeneracy, in the present simulation experiment, cumulative intensity loss (Moler & Soloman, 1970) also has been computed in the presence of IW and without IW considering the phase shift with sub-surface-duct frequency of 1031.9 Hz (Urlick, 1975) instead of individual ray paths. The anomaly explains the impact of IW on acoustic propagation characteristics in LF IW field. From the above, one can conclude that the transmission loss anomaly with reference to mean is found to be 38.4 dB. The simulation results would be found more useful in systems design of under water vehicles and basic research.

4. Conclusions

IW characteristics from insitu observations (hourly CTD data) off Paradeep, have been examined from GM model which is useful to obtain the sound velocity perturbations with space and time. The impact of IW on acoustic propagation is studied from acoustic modeling for low frequency (LF) IW field which is useful to naval operations. The computed values of period (t_{per}), velocity (c_{vel}), wavelengths (L) and wave numbers (k) are found to be 2.133 hrs – 34.72 hrs, 0.135 km hr⁻¹, 0.37 km - 6.2 km and 2.70 - 0.16 cycles km⁻¹ respectively. The semi-diurnal tidal forces are predominant than diurnal as well as other frequencies and contributing about 64 % towards total energy (E_o) of 3.34 J m⁻².

Acoustic modeling is carried out to compute transmission loss anomaly for source-receiver configuration at the depth of 53 m and range of 9 km., in the GM model generated IWs under low frequency. The loss in the acoustic propagation was found to be 38.4 dB due to the presence of LF IWs.

Acknowledgements

The authors are grateful to Dr. S.R.Shetye, Director, National Institute of Oceanography, Goa, for his keen interest in this study. Ms. Sridevi is thankful to CSIR, New Delhi for providing the Senior Research Fellowship. The authors would like to thank Naval Research Board (NRB), New Delhi for financial support. We appreciated the anonymous reviewers for their valuable suggestions which helped to improve the original manuscript.

References

- Carnahan, B., Luther, H.A. and Wilkes, J.O.: 1969, Applied Numerical methods, *John Wiley and Sons, New York. pp-604.*
- Defant, A.:1961, *Physical Oceanography*, volume 2. Oxford Pergamon Press, 517- 526.
- Desanto, J.A.:1979, *Theoretical Methods in Ocean Acoustics*, in *Ocean Acoustics* edited by Desanto J A, (Springer-Verlag, New York, 1979) pp 7-77; see also Dugan J P, *Oceanography in Under water Acoustics* Chapter 5.
- Dirk Tielburger, Steven Finette and Stephen Wolf, :1997, Acoustic propagation through an internal wave field in a shallow water waveguide, *J.Acous. Soc. Amer.*, **101** (2) 789-808.

- Dong-Jiing, Doong., Li-Chung Wu., Chia Chuen Kao.:2007, Internal Wave propagation observed by Shipboard Radar. *Sea Technology* **48**, 42- 45.
- Dozier, L.B., Tappert, D., 1978. Statistics of normal mode amplitudes in a random Ocean. I. Theory. *J,Acous.Soc.Amer* **63**, 353 - 365.
- Evans, R.B.: 1992, The existence of generalized eigenfunctions and multiple eigen values in underwater acoustics, *J,Acous.Soc.Amer.* **92**, 2024-2029.
- Flatte, M., Dashen, R., Munk, W. H., Watson, W., Zachariasen, F.:1979, *Sound Transmission through a fluctuating Ocean*, 56-57 Cambridge University Press, England.
- Garrett, C.J.R. and Munk, W.H.:1972, Space time scales of internal waves. *Geophys. Fluid Dyn.* **3**, 225-264.
- Garrett, C., and Munk, W.:1975, Space-time scales of internal waves: A progress report. *J. Geophys Res.*, **80**, 291-297.
- Garrett, C., and Munk, W.: 1979. Internal Waves in the Ocean. *Annual Reviews in Fluid Mechanics* **11**, 339-369.
- Gregg, M.C. and Briscoe, M.G.: 1979, Internal waves, fine structure, microstructure and mixing in the ocean. *Reviews of Geophysics and Space Physics* **17**, 1524-1547.
- Krishna Kumar, G.V., and Murthy, P.G.K.:1998, Internal wave characteristics in the coastal waters off Cochin in October 97, *Proc. Natl. Conf.* Current trends in the ocean prediction with special Reference to Indian seas (Dec. 22-23, Kochi, India), 90-94.
- Krishna Kumar, G.V., and Murthy, P.G.: 2002, Simulation of Sound Speed Structure due to Internal Waves In the Ocean, *Proc. ICONS – International Conference on Sonar-Sensors and Systems.*
- Krishna Kumar, G.V. and Balasubramanian, P.:2005, IWAVE: An Ocean simulation model for internal waves. *Curr. Sci.* **89**, 1927- 1932.
- Moler, C.B., and Solomon, L.P.: 1970, Use of splines and numerical integration in geometrical Acoustics. *J. Acou. Soc. Amer.* **48**, 739.
- Muller, P. and Briscoe, M.G.: 2000, Dynamical mixing and internal waves. *Oceanography* **13**, 98-103.
- Munk, W.H., Zachariasen, F.:1976, Sound propagation through a fluctuating Ocean: Theory and observations. *J. Acou. Soc. Amer.* **59**, 818-838.
- Munk, W.H., Wunsch, C.:1979, Ocean Acoustic Tomography: A scheme for large scale ocean monitoring. *Deep Sea Res.* **26**, 123-161.
- Munk, W.:1981, *In evolution of Physical Oceanography*. MIT press, Massachusetts, USA.

- Munk, W.H. and Wunsch, C.:1998, Abyssal recipes II, Energetics of the tides and wind. *Deep Sea Res.* **45**, 1976-2009
- Murthy, P.G.K. and Murthy, G.R.K.:1986, A case study on the influence of internal waves on sound propagation in the sea. *J. Sound. Vibration.* **108** (3), 447.
- Murthy, P.G.K., and Mohan Kumar, N.:1996, *Confirmatory checks for the internal waves in the coastal waters off Cochin*, Proc. Second workshop Sci. Res. FORV Sagar Sampada, pp 39-45.
- Murthy, P.G.K., and James, V.V.:1996, *Some aspects of Internal waves in the coastal waters off Cochin*, Proc. Second workshop Sci. Res. FORV Sagar Sampada, pp 47-55.
- Murthy, P.G.K.:2002, *An Insight Into Internal Waves In the Seas – around India. International Conference on Sonar – Sensors and Systems*, Proc. of ICONS, Kochi, Naval Physical and Oceanographic Laboratory, India, pp 525-532.
- Ralston, A. and Wilf, H.S.:1967, *Mathematical methods for digital computers, Spline functions, Interpolation and numerical quadrature*, T.N.E. Greville, pp 156-168.
- Ramana Murty, T.V., Prasanna Kumar, S., Somayajulu, Y.K., Sastry, J.S., Rui, J.P., De Figueiredo.:1989, Canonical sound speed profile for the central Bay of Bengal. *J. Earth. ----- Sys. Sci.*, 255-263.
- Ramana Murty, T.V. and Mahadevan, R.: 1994, Stochastic Inverse Method for Ocean acoustic tomography studies – A simulation experiment, *Technical report No. 31, Indian Institute of Technology, Madras, India.*
- Ramana Murty, T.V., , Malleswara Rao, M.M., Surya Prakash, , Chandramouli, P., and Murty, K.S.R.: 2005, Algorithms and interface for Ocean acoustic ray tracing, *Technical report No. NIO/TR-09/2005*, National Institute of Oceanography, Regional Center, Visakhapatnam, India.
- Ramana Murty, T.V., Sadhuram, Y., Malleswara Rao, M.M., Sujith Kumar, S., Maneesha, K., Sai Sandhya, K., Surya Prakash, S., Chandramouli, P., Murty, K.S.R.: 2007, Identification and Modeling of Internal Waves, *Technical report No. NIO/TR-02/2007*, National Institute of Oceanography, Regional Center, Visakhapatnam, India.
- Rao., A.D., Babu, S.V., Prasad, K.V.S.R., Ramana Murty, T.V., Sadhuram, Y., and Mahapatra, D.K.:2010, Investigation of the generation and propagation of low frequency internal waves: A case study for the east coast of India, *Est. Coast. Shelf Sci.* **88** (1) 143-152.
- Robinson A.R, and Ding Lee.:1994, *Oceanography and Acoustics*, AIP Press, pp257.
- Sridevi B., Ramana Murty T.V., Sadhuram Y., Rao M.M.M., Maneesha K., Sujith kumar S. and Prasanna P.L.: 2010, Impact of internal waves on sound propagation off Bhimilipatnam, east coast of India, *Est. Coast. Shelf Sci.* **88** (2), 249-259.

Stephen, M.Chiswell.: 2000, Tidal Enerietics over the Chatham Rise. New Zealand, *J.Phy. Oceanogr.*, pp 2452-2460.

Urick, R.J.:1975, *Principles of under water sound. 2nd ed.*, McGraw-Hill Book Company, New York. pp.384.

Xiaofeng, Li., John Morrison., Leonard Pietrafesa., Andy O Chadlick.:1999, Analysis of Oceanic Internal Waves from Airborne SAR Images. *J. Coast. Res.* **15**, 884 - 891.

Table1: IW characteristics in the coastal waters off Paradeep
(North Bay of Bengal)

Frequency (ω_i) (cph)	Period (t_{per}) (hours)	Wave length (L) (km)	Wave number (k) (cycles km⁻¹)	Potential energy (PE) (J m⁻²)	Baroclinic potential energy (BPE) (J m⁻²)
0.029	34.722	6.20	0.16	0.09415	0.02540
0.042	24.000	4.22	0.24	0.03119	0.01098
0.069	14.535	2.56	0.39	0.57329	0.01865
0.08	12.421	2.18	0.46	2.15380	0.05567
0.109	09.191	1.62	0.62	0.34851	0.01846
0.149	06.720	1.18	0.85	0.02318	0.00121
0.189	05.297	0.93	1.08	0.00621	0.00117
0.229	04.371	0.77	1.30	0.00303	0.00078
0.269	03.720	0.65	1.54	0.04523	0.00205
0.309	03.238	0.57	1.75	0.00459	0.00015
0.349	02.867	0.50	2.00	0.04523	0.00205
0.389	02.572	0.45	2.22	0.00393	0.00112
0.429	02.332	0.41	2.44	0.00414	0.00026
0.469	02.133	0.37	2.70	0.00429	0.00044
Total				3.34077	0.13839

Figure captions

Figure 1: Location of the study area (◆) for time series CTD data at 130m Off Paradeep (north Bay of Bengal)

Figure 2: Time series data on Temperature ($^{\circ}\text{C}$) off Paradeep during 24 – 25 October 2008.

Figure 3: Time series data on Salinity (psu) off Paradeep during 24 – 25 October 2008.

Figure 4: Depth - time section of Sound Velocity (m s^{-1}) off Paradeep during 24 – 25 October 2008.

Figure 5: Mean vertical distribution of temperature ($^{\circ}\text{C}$), salinity (psu), sound velocity (m s^{-1}) and Brunt-vaisala frequency (cph) off Paradeep during 24 -25 October 2008.

Figure 6: Variation of vertical displacement (m) for (a) diurnal and (b) semi-diurnal derived from CTD data .

Figure 7: (a) Amplitude and (b) Phase of IWs for various frequencies derived from time series CTD data .

Figure 8: (a) Spatial and (b) Temporal dependence of sound velocity distribution in the internal wave field off Paradeep.

Figure 9: Ray paths for (a) range independent and (b) range dependent.

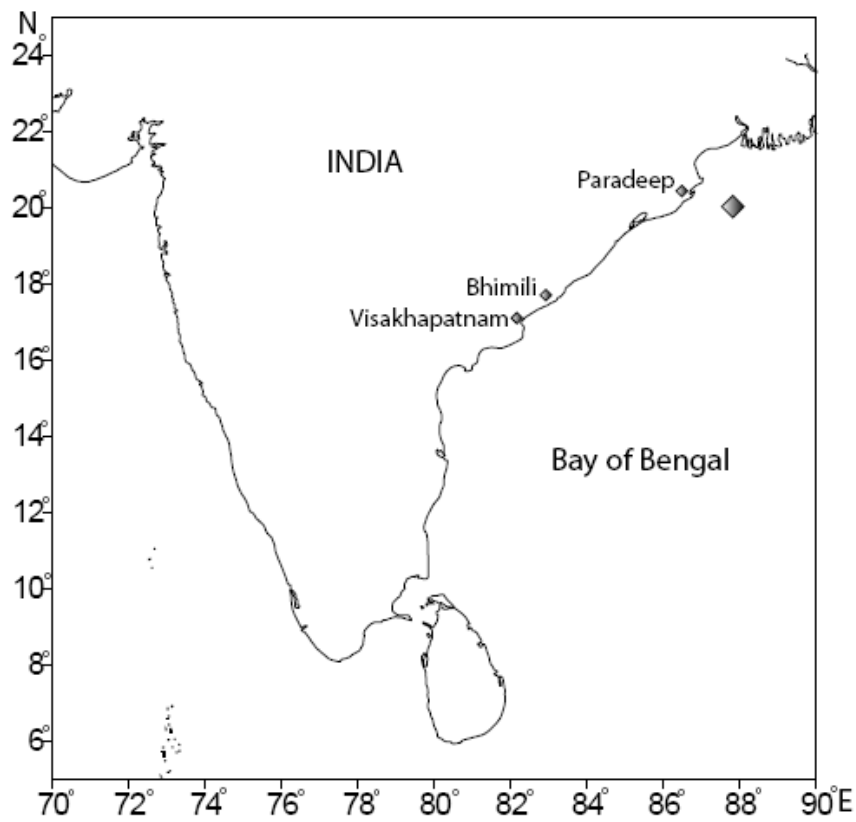


Fig 1: Location of the study area (◆) for time series CTD data at 130m Off Paradeep (north Bay of Bengal)

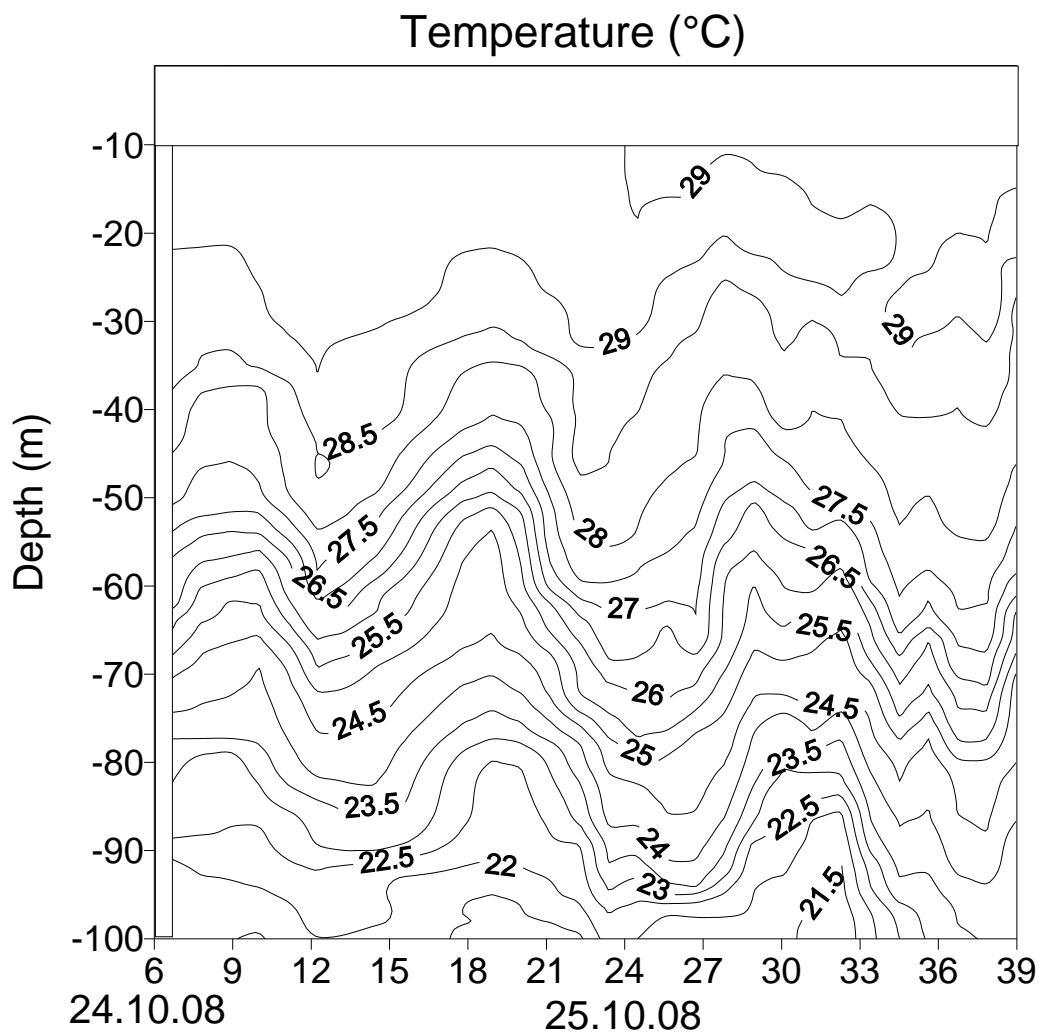


Fig 2: Time series data on Temperature (°C) off Paradeep during 24 – 25 October 2008

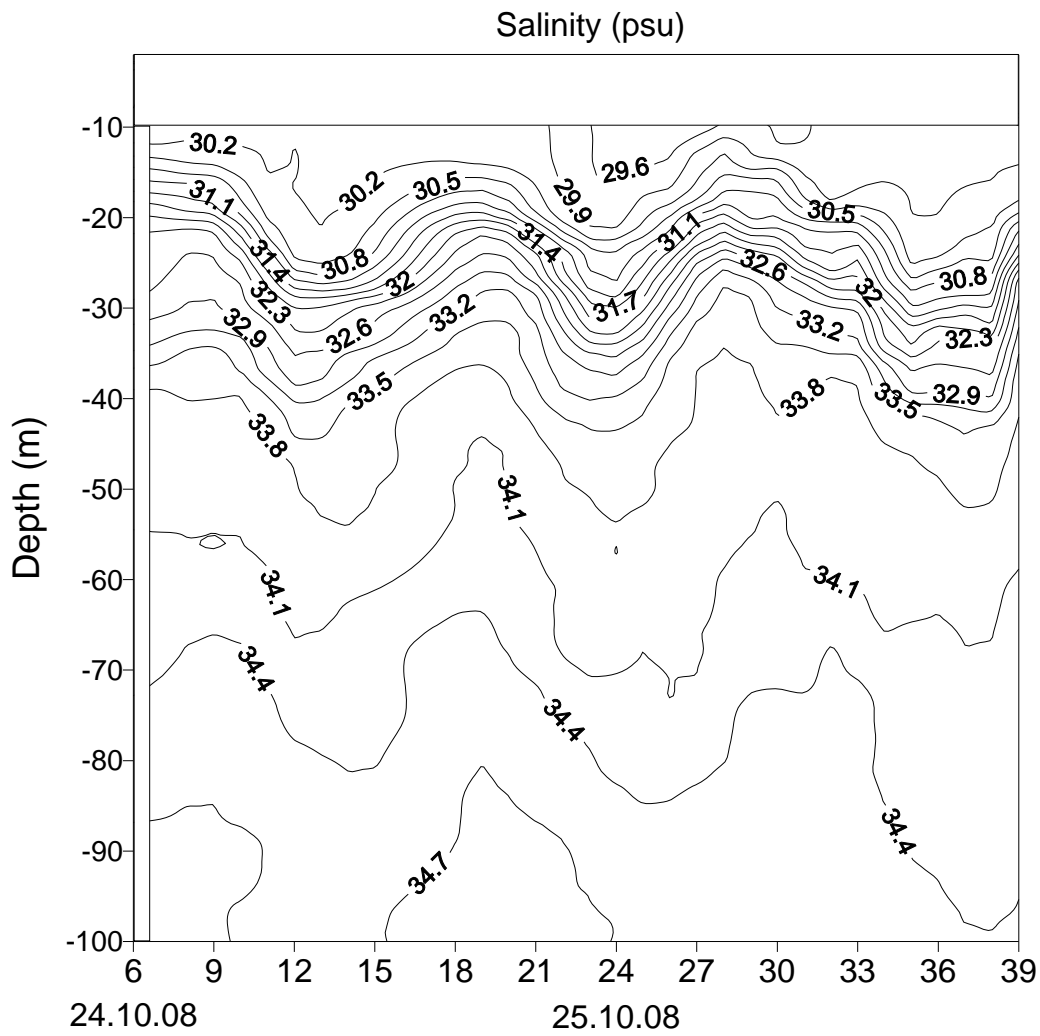


Fig. 3: Time series data on Salinity (psu) off Paradeep during 24 – 25 October 2008

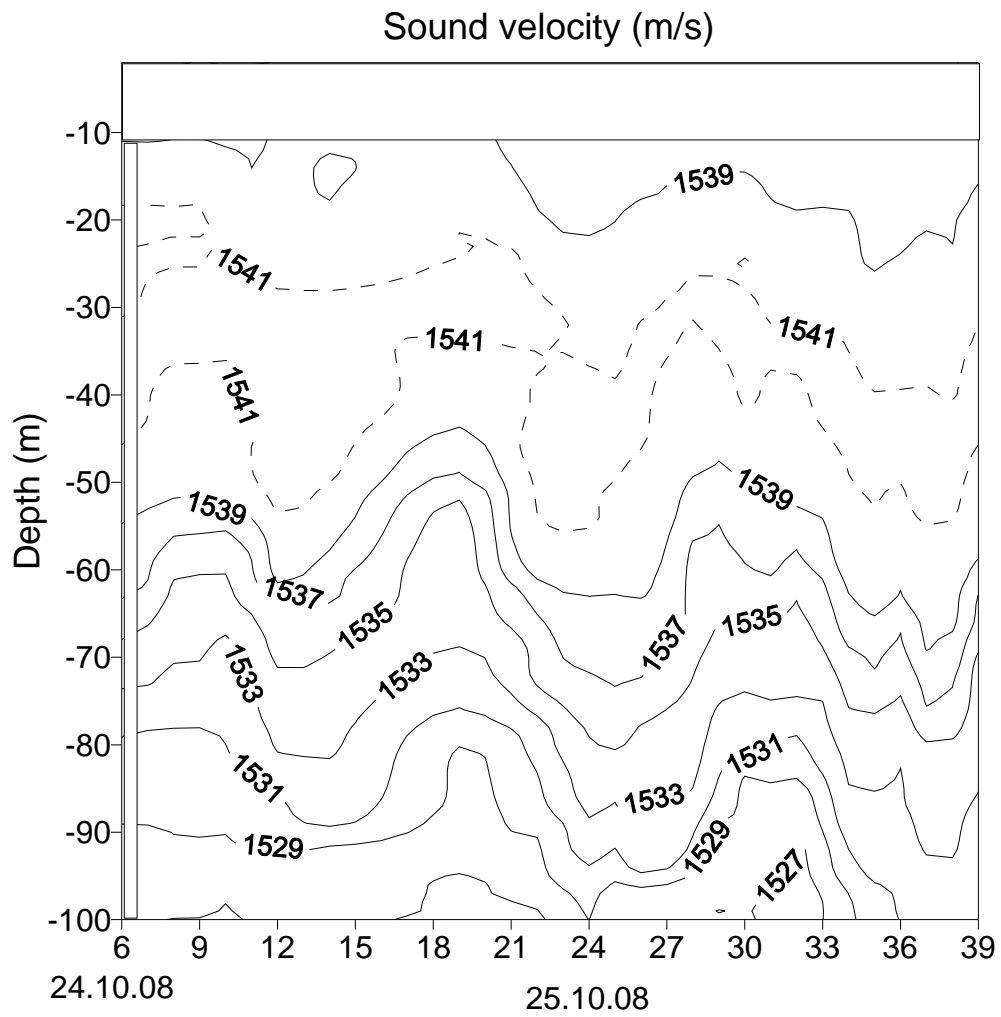


Fig. 4: Time series data on Sound Velocity (m s^{-1}) off Paradeep during 24 – 25 October 2008.

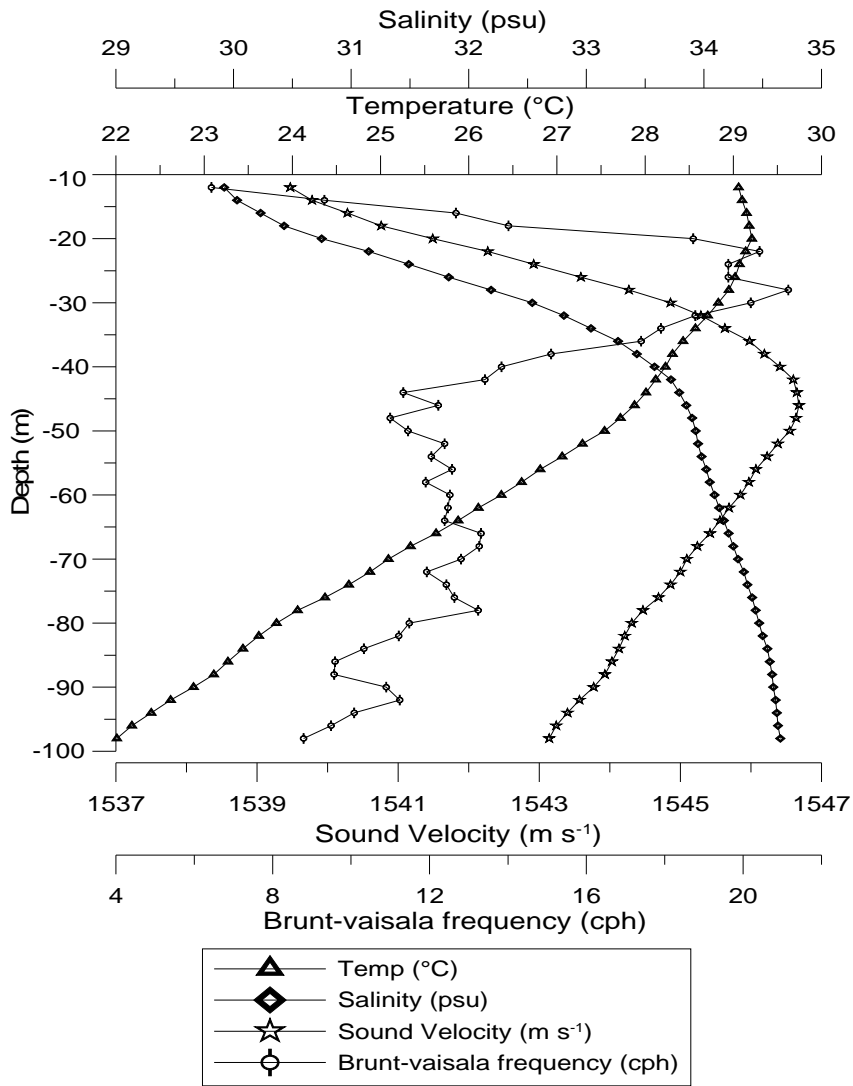


Fig. 5: Mean vertical distribution of temperature (°C), salinity (psu), sound velocity (m s⁻¹) and Brunt-Vaisala frequency (cph) off Paradeep during 24 - 25 October 2008

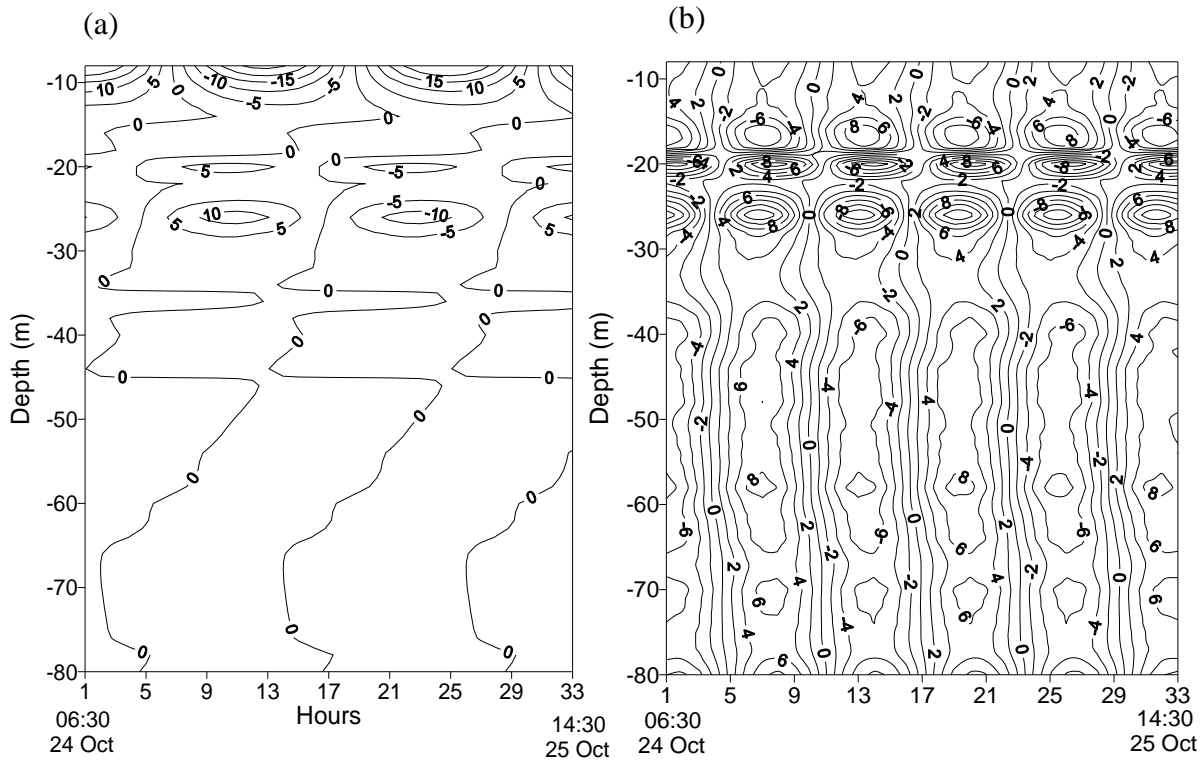


Fig. 6: Variation of vertical displacement (m) (a) diurnal and (b) semi-diurnal derived from CTD data off Paradeep.

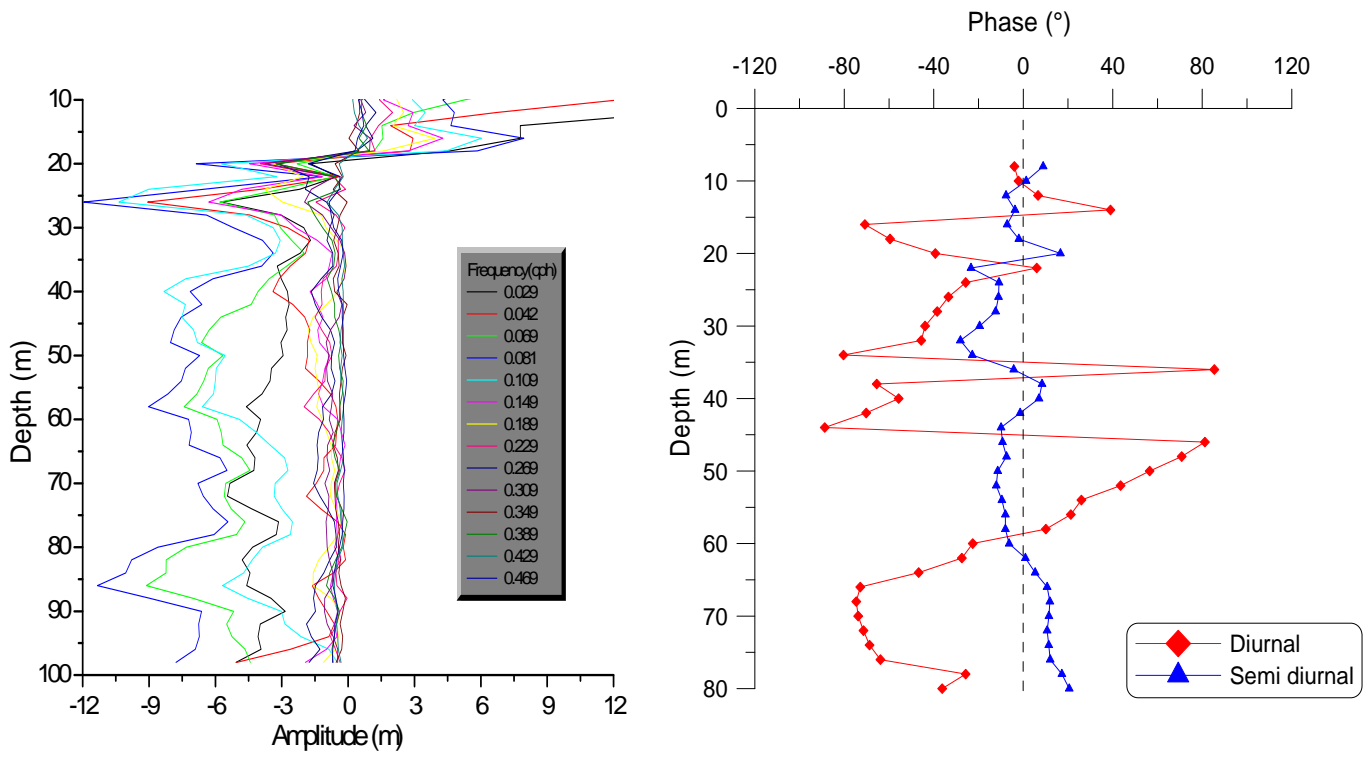


Fig. 7: (a) Amplitude and (b) Phase of IWs for various frequencies derived from time series CTD data

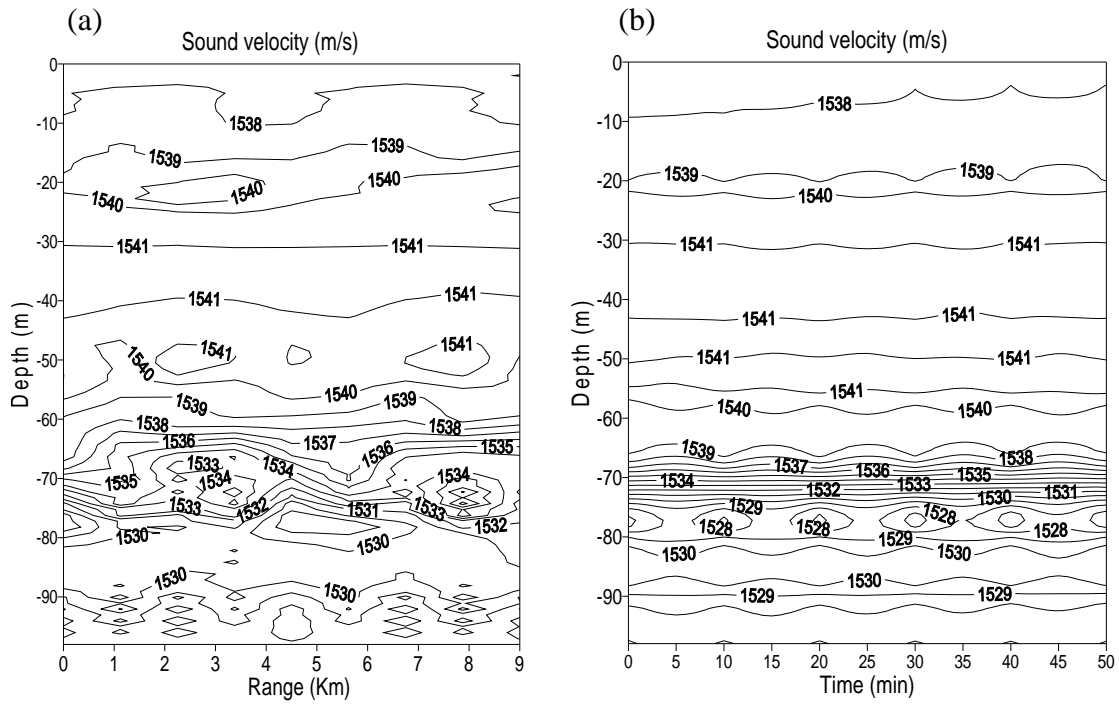
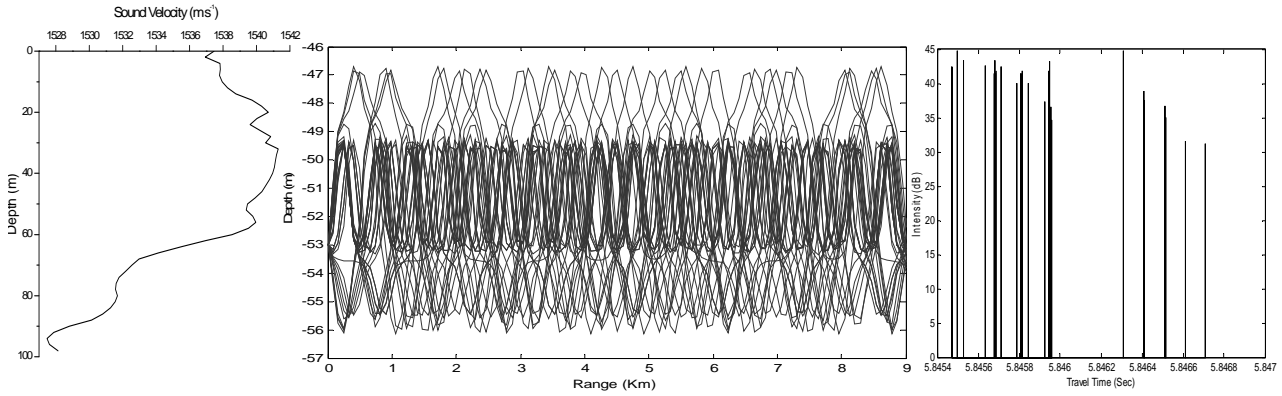


Fig. 8: (a) Spatial and (b) Temporal dependence of sound velocity distribution in the internal wave field off Paradeep

Range - independent LF IW field



Range- dependent of LF IW field

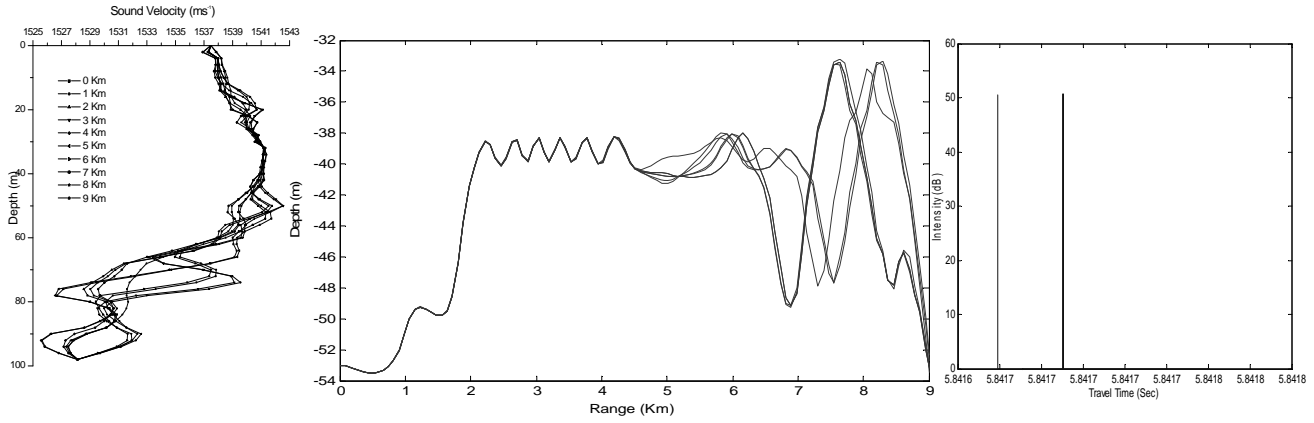


Fig. 9: Ray paths for (a) range independent and (b) range dependent